

The dense and asymmetric central star wind of the young PN He 2-138

R. K. Prinja^{1*}, S. E. Hodges¹, M.A. Urbaneja² and D. L. Massa³

¹*Dept. of Physics & Astronomy, University College London, Gower Street, London WC1E 6BT*

²*Institute for Astronomy, University of Hawaii, 2680 Woodlawn Drive, Honolulu, HI 96822, USA*

³*Space Telescope Science Institute, 3700 San Martin Drive, Baltimore, MD 21218, USA*

Accepted 2009. Received 2009; in original form 2009

ABSTRACT

We present optical *ESO* time-series and UV archival (*FUSE*, *HST*, *IUE*) spectroscopy of the H-rich central star of He 2-138. Our study targets the central star wind in a very young planetary nebula, and explores physical conditions that may provide clues to the nature of the preceding post-AGB super-wind phases of the star. We provide evidence for a dense, slowly accelerating outflow that is variable on time-scales of hours. Line-synthesis modelling (SEI and CMFGEN) of low and high ionization UV and optical lines is interpreted in terms of an asymmetric, two-component outflow, where high-speed high-ionization gas forms mostly in the polar region. Slower, low ionization material is then confined primarily to a cooler equatorial component of the outflow. A dichotomy is also evident at photospheric levels. We also document temporal changes in the weak photospheric lines of He 2-138, with tentative evidence for a 0.36-day modulation in blue-to-red migrating features in the absorption lines. These structures may betray 'wave-leakage' of prograde non-radial pulsations of the central star. These multi-waveband results on the aspherical outflow of He 2-138 are discussed in the context of current interest in understanding the origin of axi- and point-symmetric planetary nebulae.

Key words: stars: outflows – stars: evolution – stars: individual: He 2-138.

1 INTRODUCTION

There are several motivations for studying the time-variable characteristics of PN central stars (CSPN): Chandra and XMM-Newton observations are providing new perspectives on the presence of hot bubbles in planetary nebulae formed from the interaction between central star fast winds and the ambient asymptotic giant branch (AGB) phase gas (e.g. Kastner et al. 2008). The origin of the X-ray emission remains uncertain, as does the consequence of a potentially spatially clumped central star fast wind. We have previously reported on far-UV *FUSE* satellite spectroscopic time-series observations of NGC 6543 (Prinja et al. 2007); there we demonstrated in particular the incidence of coherent, systematically evolving structures in the fast wind of the H-rich central star. The empirical characteristics derived by Prinja et al. (2007) are clearly comparable to the signatures of large-scale structure in clumped radiation pressure-driven winds of OB stars. The post-AGB mass-loss via a fast wind

is important not only because of its dynamical interaction with the nebula, but also due to its effect on the evolution of the central star.

An improved understanding of the variable nature of CSPN spectral line profiles is also important in studying binarity in these objects, and thus post-common envelope evolution. In this case recorded photometric and spectroscopic signatures may be complicated by the influence of, for example, variable photospheric structure and an inhomogeneous inner stellar wind region (see e.g. De Marco et al. 2008). Furthermore, complex changes in diagnostic spectral lines can impact on non-LTE model atmosphere analyses aimed at deriving fundamental parameters of CSPN, including revisions to mass-loss rates due to strongly clumped outflows (e.g. Kudritzki, Urbaneja & Puls 2006; Urbaneja et al. 2008).

Though the UV resonance lines are undoubtedly the most appropriate for probing CSPN fast winds (e.g. Perinotto 1987), there is unfortunately a dearth of suitable UV *time-series* datasets (*IUE*, *FUSE*, or *HST*) currently available for these objects. We explore in this paper therefore the alternative of exploiting optical time-series data that offer diagnostics of variable conditions in, both, the fast wind

* E-mail: rkp@star.ucl.ac.uk (RKP); seh@star.ucl.ac.uk (SEH); urbaneja@ifa.hawaii.edu (MAU), derck.l.massa@nasa.gov (DLM)

Table 1. He 2-138 central star parameters.

Parameter	Value	Reference
Sp. type	Of (H-rich)	Mendez et al. (1998)
T_{eff}	29000 ± 1000 K	This study.
$\text{Log } g$	2.95 ± 0.15	This study
$\text{Log } (L/L_{\odot})$	3.90	This study
Distance	3.5 kpc	Zhang (1995)
Radial velocity	-49 km s $^{-1}$	Schneider et al. (1983)

and close to the stellar surface. We focus in this respect on high-quality *ESO* optical data of the young H-rich central star He 2–138.

1.1 He 2-138

This paper reports on optical time-series and archival UV data of the central star of He 2-138 (PK 320-09 1). The central star provides an interesting balance in that (i) its fast wind reveals intermediate strength, unsaturated UV resonance lines, (ii) the weaker optical photospheric lines are very symmetric and likely not ‘contaminated’ by wind effects, and (iii) the wind densities at low velocities are high enough to provide some optical signatures of the outflow. The nebula itself has a complex knotted appearance, with bubble-like structures arranged in fairly symmetrical form, providing an overall elliptical morphology (see e.g. the HST WFPC2 H α imaging survey of Sahai & Trauger 1998).

There is no recent published model atmosphere analysis of the central star, though a non-LTE study deriving a few basic parameters is given by Mendez et al. (1988); Adopted parameters are listed in Table 1 and include values derived from a new non-LTE analyses carried out during our present study of He 2-138.

Hutton & Mendez (1993) have documented visual magnitude changes in He 2-138 with amplitudes of between ~ 0.1 and 0.15 mag. The fluctuations occur over timescales of a few hours and are similar to those evident in IC 418 (e.g. Mendez et al. 1986). The magnitude changes are not obviously modulated or periodic and may relate to variable conditions in the near-photospheric (inner-wind) regions. In their search for radial velocity variations in Southern Hemisphere CSPN, Afar & Bond (2005) quote a greater than 99% probability that He 2-138 is a radial velocity variable. These changes occur over \sim daily time-scales, but without any convincing evidence for a period.

Our aim in this study is to determine optical and UV mass-loss parameters for an object that is in the early stages of the planetary nebula phase. We explore here the evidence for a structured outflow in He 2-138 and examine corresponding or unrelated signatures for photospheric variability.

2 ESO TIME-SERIES OPTICAL SPECTROSCOPY

The study of variability in the central star of He 2-138 is based primarily on data collected from the ESO 3.6m telescope at La Silla, with the HARPS spectrograph, over three nights between 2006 March 24 and March 26

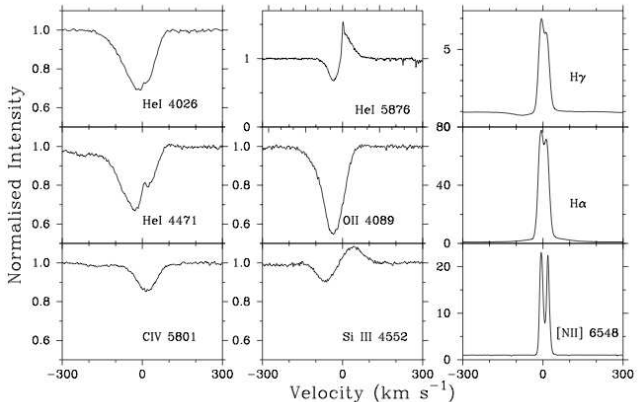


Figure 1. Mean ESO optical spectral lines of photospheric (left-hand panels), central star wind (middle panels) and nebular signatures (right-hand panels) in He 2-138.

(BJD 2453818.67601 to 2453820.90567). During each of the three nights 6 spectra were secured over a time span of ~ 5.5 hours. The HARPS instrument delivered a total spectrum range of ~ 4000 to 7000\AA , with spectral resolution $R \sim 110,000$. The continuum signal-to-noise in individual spectra, achieved in 30 minute exposures, is typically ~ 40 . Standard ESO pipe-line data reduction was conducted using MIDAS procedures, including flat-fields, bias subtraction and wavelength calibration. All spectral line profiles presented here have been corrected for a system radial velocity of -49 km s $^{-1}$ (e.g. Table 1).

The typical spectrum includes stellar lines plus nebular emission. Characteristic features spanning near-photospheric He I and weak metal line absorption profiles; blue-shifted absorption and weak P Cygni lines; and nebular lines are shown in Fig. 1. The stellar continuum is derived by fitting line-free regions of the spectrum with a first-order polynomial; this study is focused on the properties of normalised line profiles and we do not attempt to derive any flux calibrated measurements. Though the spectra have been secured in varying seeing conditions and position angles, the primary line profile changes studied here can be attributed to stellar variations. The nebular lines (e.g. [NII] in Fig. 1) confirm that He 2-138 is a low excitation planetary nebula.

3 TIME-AVERAGED FAST-WIND CHARACTERISTICS

We collate in this section the overall *mean* outflow properties of He 2-138, based on our ESO optical dataset and archival UV spectra. Additional fundamental parameters are also derived here from non-LTE line-synthesis modelling of the time-averaged spectra.

The fast wind of He 2-138 is most sensitively diagnosed in the optical time-series primarily by a well developed P Cygni-like profile in He I $\lambda 5875.57$ ($2^3\text{P}^0 - 3^3\text{D}$). The blueward absorption trough extends to ~ -200 km s $^{-1}$, with comparable redward extent for the emission wing. This line serves as the most useful probe of temporal behaviour in the fast wind and its variability signatures are derived in Sect. 4.

Additional information on the nature of the fast wind in

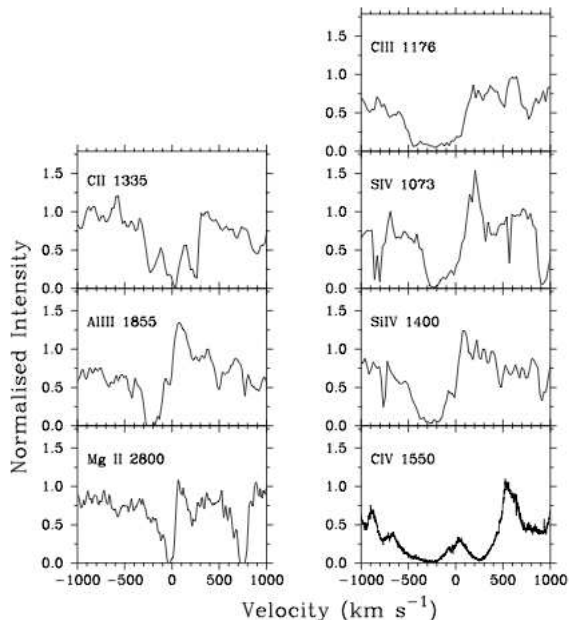


Figure 2. *FUSE*, *IUE* and *HST* spectral lines that provide UV signatures of the fast-wind in He 2-138.

He 2-138 can be extracted from UV data. A selection of the wind-formed line profiles in *FUSE*, *IUE*, and *HST* spectra is shown in Fig. 2. The wind is evident in low-ionisation species due to C II λ 1335, Al III $\lambda\lambda$ 1855, 1863, Mg II $\lambda\lambda$ 2796, 2802, and also in the higher ions Si IV $\lambda\lambda$ 1063, 1073, Si IV $\lambda\lambda$ 1394, 1403, and C IV $\lambda\lambda$ 1548, 1551. Note that N V $\lambda\lambda$ 1238, 1242 and O VI $\lambda\lambda$ 1032, 1038, which generally trace shocked gas in hot star winds, is absent in He 2-138. The blueward absorption trough of the high-ion lines extend to ~ 500 to 700 km s $^{-1}$, and ~ 100 to 300 km s $^{-1}$ in the low ion species. Overall, the wind lines exhibit strong optical depths, including saturated regions at low to intermediate velocities.

The impression from the UV lines and a P Cygni-like He I λ 5876 is that He 2-138 has a dense, comparatively slow central star wind. Further support is provided by the unusual behaviour of the Si III λ 1300 triplets shown in Fig. 3, where the rest wavelengths of the lines are indicated in the radial velocity corrected *IUE* spectrum. The Si III triplets are clearly blueshifted by between -60 km s $^{-1}$ to -80 km s $^{-1}$ and thus trace the radial expansion at the base of the outflow. We conclude that a very dense, slowly accelerating wind is implied in these data.

3.1 Line-synthesis modelling

To decode physical parameters from the UV wind resonance lines we first employed the ‘Sobolev with exact integration’ (SEI) code of Lamers et al. (1987), but with modifications detailed in Massa et al. (2003); these changes principally permit the radial optical depths of the wind to be treated as independent, discrete and variable bins in velocity space. Once the empirical velocity law of the wind is determined, this approach provides reliable radial optical depths for unsaturated wind lines as a function of normalized velocity, $\tau_{rad}(w)$, where $w = v/v_\infty$ and v_∞ is the terminal velocity

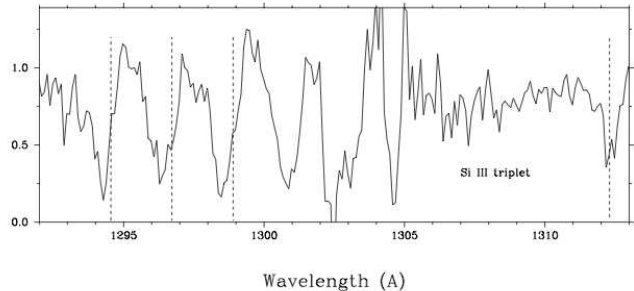


Figure 3. Blueward shifted Si III λ 1300 triplets in the UV spectrum of He 2-138. The Si III singlet at λ 1312 is also shown for comparison. The vertical dashed lines mark the rest positions.

Table 2. SEI-derived mass-loss and wind ionization parameters.

Ion	$\langle \dot{M} q_i \rangle$ ($M_\odot \text{ yr}^{-1}$)	$\langle q_i \rangle$
C $^{3+}$	6.9×10^{-11}	6×10^{-4}
Si $^{3+}$	1.7×10^{-10}	1×10^{-3}
S $^{3+}$	2.4×10^{-9}	2×10^{-2}
Al $^{2+}$	5.5×10^{-10}	5×10^{-3}
C $^{+}$	1.1×10^{-11}	9×10^{-5}

of the wind. The fits to individual wind lines require parameters for the terminal velocity, ‘ β -type’ velocity law, turbulent velocity, and $\tau_{rad}(w)$ (specified as a set of 21 independent velocity bins). The effect of a photospheric spectrum in the SEI profile fitting is approximated by adopting a TLUSTY plane-parallel model atmosphere spectrum (Hubeny & Lanz, 1995) for $T_{\text{eff}} = 29000$ and $\log g = 3.0$ and a projected rotation velocity of 45 km s $^{-1}$ (see below and Table 1). This input photospheric spectrum provides a reasonable match to the ‘underlying’ absorption and it primarily needs to be incorporated to match wind-formed profiles that are located across the heavily line-blanketed UV regions between $\sim 1300\text{\AA}$ to 1900\AA . The $\tau_{rad}(w)$ values were converted into a product of \dot{M} times ionization fraction, $\dot{M} q_i(w)$ (see, e.g., Massa et al. 2003); we derive here the mean $\langle \dot{M} q_i \rangle$ values over $0.2 \leq v/v_\infty \leq 0.9$ for several ions analysed.

SEI model fits to Si IV $\lambda\lambda$ 1400 (*IUE*), C IV $\lambda\lambda$ 1400 (*HST*), Si IV λ 1073 (*FUSE*), and Al III $\lambda\lambda$ 1855, 1863 (*IUE*) are shown in Fig. 4, and include panels displaying the TLUSTY photospheric inputs and the derived radial optical depths as function of normalised velocity. We note firstly that reasonable matches to the observed data are obtained, but we require a different maximum velocity for Si IV and C IV ($= 750$ km s $^{-1}$) as opposed to 300 km s $^{-1}$ for Si IV and the low ion species generally. For an assumed solar abundance and parameters adopted in Table 1 (and derived below), the values obtained for the product of mass-loss rate and ionization fraction ($\langle \dot{M} q_i \rangle$) are listed in Table 2.

Despite the slow velocity law used ($\beta = 3$) and generally high turbulent velocities (v_t), the SEI models mostly underpredict the strengths of the emission components. Additionally, the fit to the C IV doublet remains problematic, where the redward low-velocity absorption component is also too

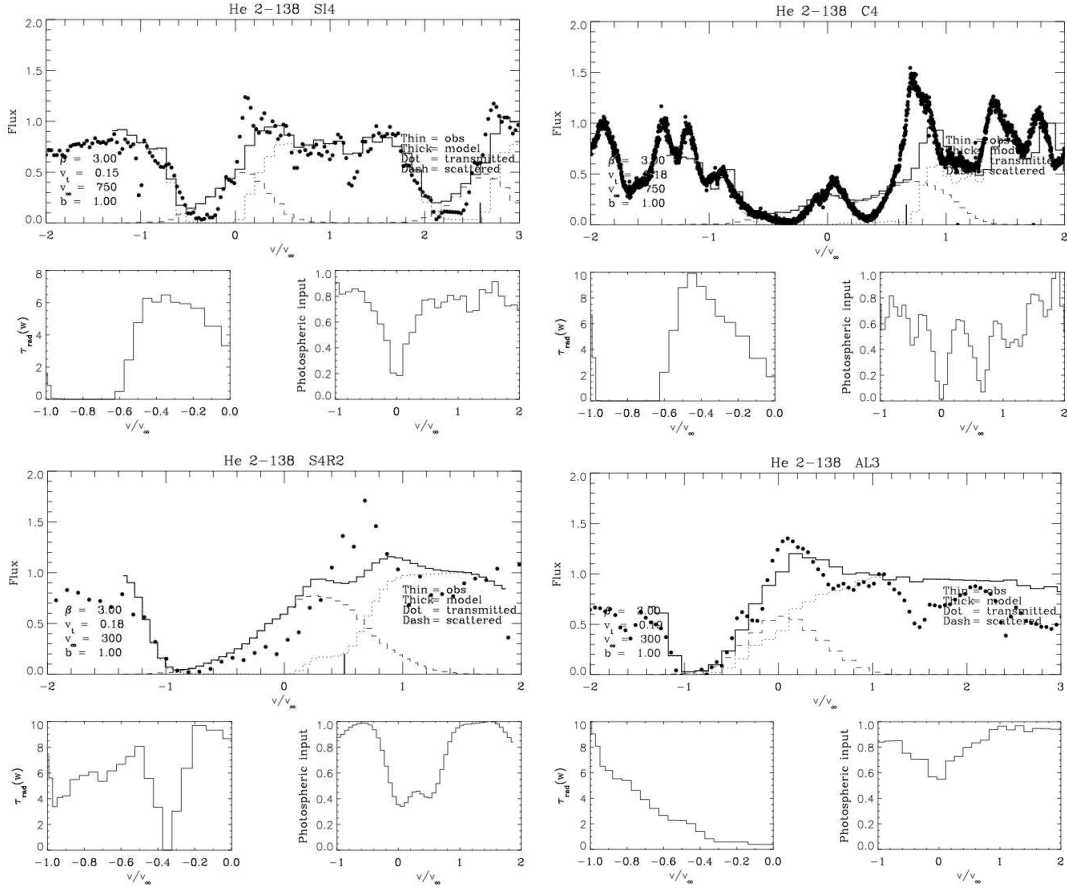


Figure 4. SEI model fits (solid line) to SiIV $\lambda\lambda 1400$ (*IUE*), CIV $\lambda\lambda 1550$ (*HST*), SiV $\lambda 1073$, and AlIII $\lambda 1855$ (*FUSE*) P Cygni profiles of He 2-138. The panels below each fit show the adopted radial optical depths and input (TLUSTY) photospheric spectra. Note that the maximum velocity adopted in SiV and AlIII of 300 km s^{-1} has to be raised to 750 km s^{-1} to match the blue wings of SiIV and CIV

weak in the model. It is also unexpected to note the large differences between the SiIV $\lambda\lambda 1063$, 1073 and SiIV $\lambda\lambda 1394$, 1403 lines, given that the ionization ranges of these lines bracket each other so closely (though the Si line has greater cosmic abundance). These discordances (Fig. 4) may confirm our conclusion earlier that He 2-138 has a very dense wind. It might in fact be that the density of the wind is so high (with a very shallow velocity law) that the Sobolev (single scattering) theory is no longer valid and the normal SEI source function is not appropriate in this case.

To gain further insights into the time-averaged characteristics of the wind, we also examined line synthesis using the unified non-LTE, line blanketed model atmosphere code CMFGEN (e.g. Hillier & Miller 1998). Very briefly, CMFGEN solves the non-LTE radiation transfer problem assuming a chemically homogeneous, spherical-symmetric, steady-state outflow. Each model is defined by the stellar radius, the luminosity, the mass-loss rate, the wind terminal velocity (v_∞), the stellar mass, and by the abundances of the species included in the calculations. The code does not solve for the hydrodynamical structure, hence the velocity field has to be defined. A solution, commonly adopted, is to use the output of a plane-parallel model (such as TLUSTY) to define the pseudo-static photosphere, connected just below the sonic point to a beta-type velocity

law to describe the wind regime. We consider H, He I/II, C II/III/IV, N II/III/IV/V, O II/III/IV/V, Mg II/III, Al III/IV, Si III/IV, P IV/V, S II/IV/V/VI and Fe III/IV/V/VI/VII in our models.

The ionization balance of He is used to derive the effective temperature. We consider only HeI lines belonging to the triplet spin system and HeII lines present in the optical spectrum. In this case, the HeII lines react strongly to changes of $\pm 1000 \text{ K}$, whilst the HeI lines remain unaffected. The surface gravity is determined by fitting the H Balmer lines series. We give more weight to higher lines in the series, because the effect of the stellar wind and the contamination by the ionized gas is less important. It has to be noted that the photospheric structure is linked to the stellar mass, hence its adopted value could produce changes. These would be very small, however, for our target object.

As shown in Fig. 5, our final model (Table 3) reproduces well most of the features present in the FUV/UV spectrum. However, the model does not match the wide absorption troughs observed in the Si IV and C IV UV profiles, and it under-predicts the strength of the Al III lines. Low ionization species present in the UV range, such as C II and Al III will require a lower (significantly lower in the case of the C features) effective temperature, but will then not reproduce the observed He I/II ionization balance. Similarly, high ion-

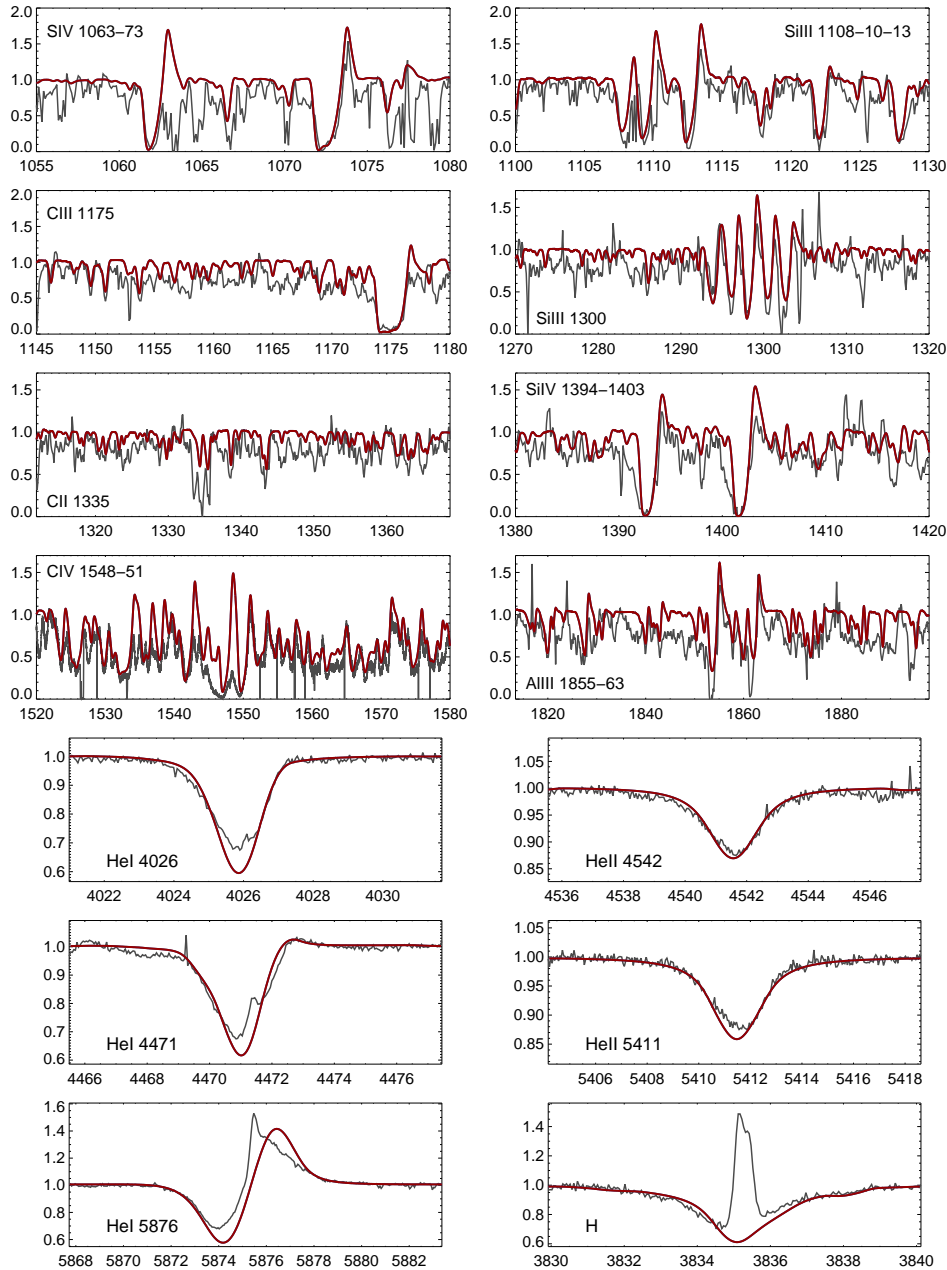


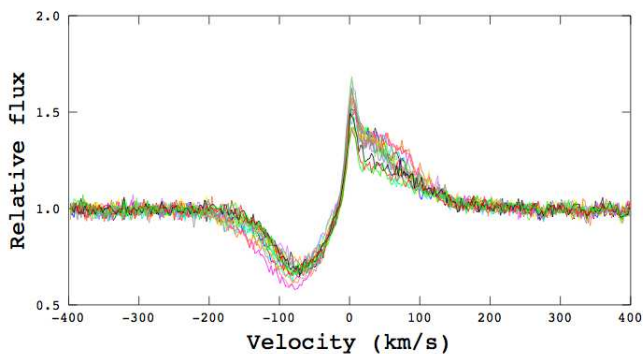
Figure 5. CMFGEN non-LTE multi-line fit (red line; Table 3) to strategic UV and optical spectral feature of He 2-138. This low terminal velocity case ($v_{\infty} = 300 \text{ km s}^{-1}$) provides a suitable match to the FUV and low ionization lines, but the model cannot adequately reproduce the strong SiIV and CIV resonance lines.

ization features present in the optical spectrum (O III and C IV lines) would require a higher effective temperature, that again would not be consistent with the He ionization balance. We noted the same discrepancy in the SEI modelling earlier (Fig. 4), where a 'two component' wind was invoked and $v_{\infty} = 750 \text{ km s}^{-1}$ used for the C IV and Si IV *IUE* lines. Note that the *HST* STIS spectrum of CIV modelled in Sect. 3.1 (Fig. 4) was secured in 2004 June and is broadly similar to the *IUE* high-resolution line profile taken in 1989 May. The maximum epoch to epoch change evident in the archival data is $\sim 100 \text{ km s}^{-1}$ in the shallow blueward wing. The variation is thus not sufficient to account for the two component behaviour discussed above.

Overall, the unusual nature of the wind lines in He 2-138 is borne out by our comparisons to the model line profiles for spherically symmetric winds. We believe that the dichotomy in matching low and high ion lines, including discrepancies (with respect to symmetric models) in the relative absorption and emission strengths of the P Cygni profiles, argue in favour of a wind whose terminal velocity and mass-loss have a latitude dependence. Low velocity, low ion species would form primarily in the cooler equatorial regions of an asymmetric outflow that is viewed almost pole-on. The high speed SiIV and CIV bearing gas is then driven out mostly in the hotter polar regions of the flow. This notion of a

Table 3. CMFGEN best solution parameters.

Parameter	Value
T_{eff}	29000 ± 1000 K
$\text{Log } g$	2.95 ± 0.15
$\text{Log } (L/L_{\odot})$	3.90
$N(\text{He})/N(\text{H})$	0.20
$\log Q$	-11.45
\dot{M}	$1.23 \times 10^{-7} M_{\odot} \text{ yr}^{-1}$
Chem. composition	solar

**Figure 6.** Variability evident in the 18 *ESO* He I 5876 P Cygni profiles of He 2-138, over ~ 2.2 days.

two-component, asymmetric wind in He 2-138 is discussed further in Sect. 5

For a v_{∞} of 300 km s^{-1} , $T_{\text{eff}} = 29000$ K, adopted central star mass of $\sim 0.6 M_{\odot}$ and a $\log (L/L_{\odot}) \sim 3.9$, the model in Fig. 5 yields a mass-loss (wind strength) parameter $\log Q \sim -11.45$ dex (where $Q = \dot{M}(R_{\star}v_{\infty})^{-1.5}$) and thus a mass-loss rate of $\sim 1.2 \times 10^{-7} M_{\odot} \text{ yr}^{-1}$. The adopted model is for a smooth wind and any clumping is unconstrained here, but it is noted as being at a very low degree. The corresponding wind momentum value $\log (\dot{M} v_{\infty} R_{\star}^{0.5})$ of ~ 26.6 dex sits within the scatter in the wind-momentum luminosity relation observed for CSPN and predicted by the line-driven wind theory (see e.g. Kudritzki, Urbaneja & Puls, 2006). Though these authors note that in the luminosity regime restricted to CSPN (and excluding luminous O-type stars), there is no convincing relation between wind momentum and luminosity.

It is interesting to compare this result from the *ab initio* CMFGEN prediction to the empirical, SEI-derived $\langle \dot{M} q_i \rangle$ results presented earlier. For a mass-loss rate of $\sim 1.2 \times 10^{-7} M_{\odot} \text{ yr}^{-1}$, the corresponding mean ion fractions based on the SEI profile fits (Fig. 4) are also listed in Table 2. The empirical analyses would suggest therefore that none of these strongly absorptive ions are dominant in the outflow of He 2-138. We note however that the CMFGEN base model (Table 3) predicts (for smooth or weakly clumped winds) that the S^{3+} and Si^{3+} ionization fractions are dominant in the wind (i.e. $\sim 90\%$). This disparity would suggest that either the CMFGEN derived mass-loss rate is overestimated or the SEI product of $\dot{M} q_i(w)$ is underestimated.

4 TEMPORAL CHANGES IN THE WIND AND PHOTOSPHERE

The time-dependent nature of the central star wind in He 2-138 is discussed here, based primarily on the *ESO* time-series data of the P Cygni-like He I 5876 feature (see Fig. 1). We also comment on additional changes noted in the deep-seated, photospheric dominated, optical lines due to He I and C IV 5801. Unfortunately there is no appropriate FUV or UV time-series dataset currently available for He 2-138. We examined the fragmented sample of 12 *FUSE* (LWRS) spectra present in the archive, covering epochs in 1999 September, 2000 March, 2000 July, 2002 April, 2007 February and 2007 April. There is no evidence for substantial blueward variability in for example the Si IV, P V or C III lines. The maximum discernible change is a $\sim 60 \text{ km s}^{-1}$ shift in the blue wing of Si IV 1073.5.

Unambiguous evidence for changes in the central star wind comes from the He I 5876 line. The sequence of 18 spectra secured over ~ 2.2 days is shown in Fig. 6. The absorption trough is variable out to $\sim 200 \text{ km s}^{-1}$. The equivalent widths vary between $\sim 0.37 \text{ \AA}$ to 0.65 \AA and $\sim 0.47 \text{ \AA}$ to 0.8 \AA , for the absorption and emission components, respectively. These changes are correlated such that the deepest absorption troughs are accompanied by the strongest emission components. At its greatest, the absorption and emission equivalent widths of the profile can increase (in concert) by $\sim 60\%$.

The temporal characteristics of He I 5876 line profile are explored further in Fig. 7, together with the properties of the photospheric dominated absorption lines of He I 4026, He I 4471, and C IV 5801. The Temporal Variance Spectrum (TVS; e.g. Fullerton et al. 1996) indicates a slight blueward asymmetry in the profile changes of He I 5876 at the 95% significance level. A strong absorption enhancement is evident during the second night of observations, extending to $\sim 200 \text{ km s}^{-1}$. These data are not intensive enough to conclude whether this is an episodic migrating feature akin to the discrete absorption components (DACs) seen generally in the UV spectra of OB stars and also reported in the *FUSE* data of NGC 6543 by Prinja et al. (2007). The weaker photospheric lines are also undoubtedly variable on hourly time-scales and the grayscale representations in Fig. 7 reveal similar systematic changes in each of three lines considered. The equivalent widths of the photospheric lines are not conserved, and we measure changes of up to $\sim 25\%$ in the He I 4471 and He I 4026 spectra. These variations do not correlate with the blueward or redward fluctuations of the He I 5876 P Cygni profile. The same is true for the very weak and narrow Si III $\lambda\lambda 4552, 4567$ and 4574 triplet shown in Fig. 1, which exhibits \sim hourly changes that mimic those of He I 4471 and He I 4026. We conclude that temporal changes in the central star wind are not evident in the deep-seated regions close to the photosphere and likely arise further out in the outflow, where they are diagnosed via He I 5876.

In Fig. 7, the data of photospheric lines, which are shown as residuals from the mean profiles, reveal blue to red travelling pseudo-absorption and pseudo-emission features in the dynamical spectra. This behaviour may be indicative of the presence of prograde non-radial pulsations of the photosphere. The variability pattern is similar from night to night. In each of the photospheric lines the redward

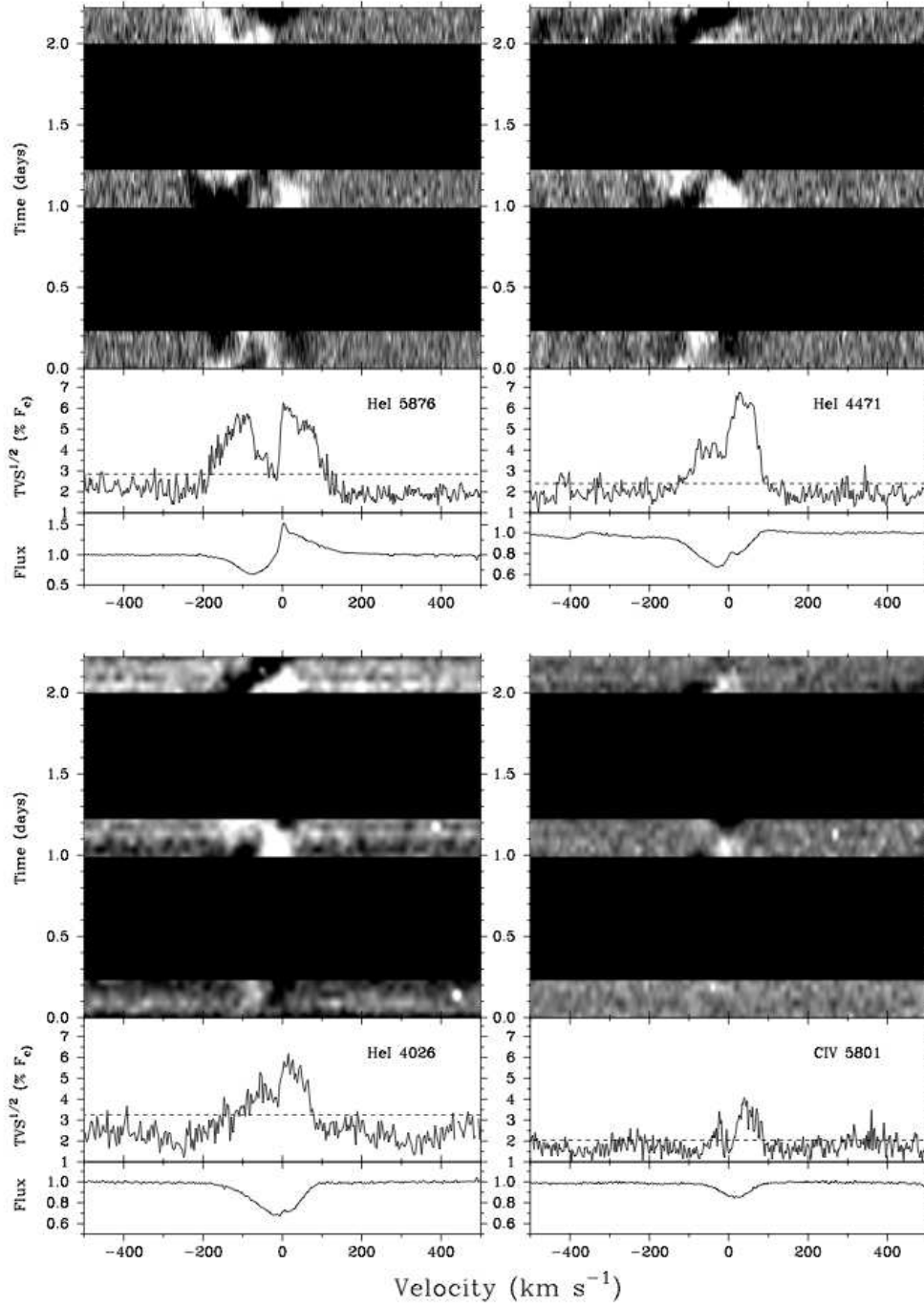


Figure 7. Temporal characteristics of the wind dominated He I $\lambda 5876$ and photospheric He I $\lambda 4026$

, He I $\lambda 4471$ and C IV $\lambda 5801$ lines. The grayscale images show temporal changes in individual spectra normalised by the mean profile shown at the bottom for each line. The dynamical range shown is 0.96 (black) to 1.05 (white). The middle panels for each line provide the variance statistic, where we highlight changes above the 95% significance level (dotted line).

variance (TVS) is stronger than the blueward TVS, and this asymmetry is marked by a drop in variance at rest velocity. The blue-to-red features migrate across the full span of the absorption trough over an estimated ~ 0.3 to 0.4 days. The empirical changes in the near-surface lines of e.g. He I $\lambda 4471$, He I $\lambda 4026$ and C IV $\lambda 5801$ are characterised by localised structure in the absorption troughs as opposed to

whole-scale radial velocity shifts about line centre. These sub-features can have the effect of extending either the blue or red wing of the profile, while the other wing stays constant. In extreme the features can result in a $\sim 25\%$ change in equivalent width. Note that though the variations in He I $\lambda 4471$ and He I $\lambda 4026$ (and other similar features in the optical spectrum of He 2-138) extend to more than ± 100 km

s^{-1} (Fig. 7), the basic pattern of changes is the same as that evident in Civ $\lambda 5801$, which is a much narrower line (closer to \pm projected rotation velocity) and likely forms very close to or at the photosphere.

With the caveat that our time-series dataset of He 2-138 is sparse, we conducted a periodogram analysis to search for evidence of cyclic behaviour in the HeI $\lambda 4026$ and HeI $\lambda 4471$ lines. The frequency range sampled by the data from $\sim 0.5 \text{ days}^{-1}$ to 10 days^{-1} was examined for periods by employing the CLEAN algorithm described by Roberts et al. (1987). Following an iterative deconvolution of the (strong) window function for our dataset, the only potentially significant peaks in the resulting power spectra are aliases of each other at $\sim 1.4 \text{ d}^{-1}$ and 2.8 d^{-1} (see Fig. 8). We estimate a $\sim 30\%$ uncertainty in these frequencies based on the widths of the power spectra features. The shorter corresponding period, i.e. 0.36 days, is repeated over more than six cycles during the full span of the observing run. Grayscale representations of the 18 individual quotient (with respect to the mean) line profiles are shown phased on the 0.36 day period in Fig. 9 (folded over 2 cycles). The HeI $\lambda 4026$ and HeI $\lambda 4471$ lines clearly show some coherency in the travelling features over the 0.36 day time-scale. In contrast the outflow dominated HeI $\lambda 5876$ profile is more fragmented in the phased plots and there is certainly no evidence that the outflow changes are modulated on this time-scale.

The detection of a residual variability pattern in Figs. 7 and 9 that extends to velocities higher than the mooted projected rotation velocity may be interpreted in terms of the 'wave-leakage' mechanism, which permits pulsations to initiate perturbations in the deepest stellar wind regions. For example, Cranmer (1996) and Townsend (2000) argue that pulsations arising in the stellar interior can migrate toward the outer atmospheric layers as high frequency gas pressure (p mode) waves or as lower frequency (g mode) waves. The notion of wave-leakage in He 2-138 would be consistent with our conclusion in Sect. 3.1 that the central star has a very dense wind, thus in effect there is no clear boundary at which pulsations get reflected and confined.

5 DISCUSSION

We have revealed that He 2-138 has a dense, slowly accelerating central star wind, that is variable on time-scales of hours to days. The SEI and CMFGEN line synthesis models presented here support the notion that He 2-138 exhibits a 'two-component' outflow: A hotter (i.e. $> 29,000 \text{ K}$) component provides a better match to the (near) photospheric Civ and OIII optical lines, but predicts too much HeII and hence less HeI. In contrast cooler models ($\sim 25,000 \text{ K}$) reproduce better the low-ionization UV lines (including CII and AlIII), but these models predict too much photospheric HeI and too weak HeII lines. Additionally, the spherically symmetric SEI and CMFGEN models cannot reproduce the observed relative absorption and emission strengths of the SiIV $\lambda\lambda 1400$, Civ $\lambda\lambda 1550$, and MgII $\lambda\lambda 2800$ P Cygni profiles. This discordance may be interpreted to suggest that the outflow is asymmetric. While the UV SiIV $\lambda 1073$ line is (a lower abundance) surrogate to SiIV in the range of ionization potential, its line profile can only be matched by adopting a maximum wind velocity of 300 km s^{-1} , while a higher velocity of 750

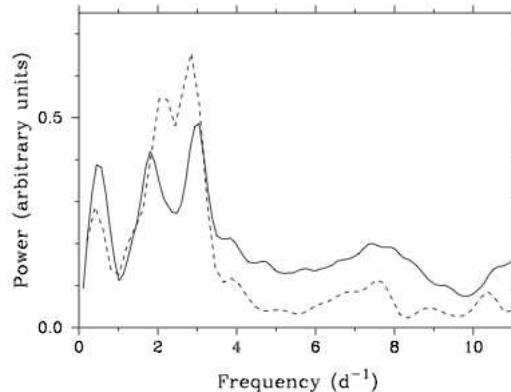


Figure 8. Power spectrum (in arbitrary units) for HeI $\lambda 4026$ (solid line) and HeI $\lambda 4471$ (dashed line). The strongest peaks correspond to (alias) signals at ~ 0.36 days and 0.72 days.

km s^{-1} is needed for SiIV $\lambda\lambda 1400$ (and Civ $\lambda\lambda 1550$). Though the spectral lines we considered have been secured at different epochs (for *ESO*, *IUE*, *HST*, and *FUSE* data), multiple archival FUV and UV spectra spanning several years do not provide any indication that the shortward wings of the wind lines are variable by several 100 km s^{-1} .

An analogous example of a 'hybrid' wind may be that of B[e] stars, where a two-component stellar wind model has been proposed (e.g. Zickgraf et al. 1985). In this scenario a hotter and faster polar wind gives rise to more extended high-excitation absorption features, and in contrast a slowly accelerating cooler equatorial disk wind promotes narrower low-excitation lines. Extremely slow (less than 100 km s^{-1}) disk winds can then be seen in B[e] stars viewed edge on. The increasing maximum outflow velocity in He 2-138 from AlIII to SiIV, and to SiIV and Civ may reflect the spatial distribution of these ions in a hypothesised latitude dependent outflow viewed approximately pole-on. One inconsistency in comparison to B[e] star-type hybrid winds is that the NV $\lambda\lambda 1240$ doublet would in this scenario be expected to be strongly in emission. This resonance line is however absent in *IUE* spectra of He 2-138, and since *FUSE* data *do* reveal the presence of NIII $\lambda 955$, we do not anticipate a strong N abundance anomaly. The absence of NV may instead reflect a general lack of shocked X-ray emitting gas. The OVI $\lambda\lambda 1032$, 1038 doublet is also not present. N^{2+} is then expected to be a dominant ionisation stage in the wind.

In addition to a proposed non-spherical outflow in He 2-138, our analyses also provides indications of some dichotomy in the photospheric lines (see above). One possibility is that the central star is a rapid rotator, and we are indeed viewing it almost pole on (i.e. at a smaller projected velocity). The rapid rotation distorts the surface layers sufficiently such that we view a hotter polar region and cooler equatorial surface.

Evidence for asymmetries in the central star wind of a very young PN such as He 2-138 is interesting in connection to the wider debate as to the origin of commonly seen, non-spherical nebulae, many of which reveal axi- and point-symmetries. For example, the higher mass-loss superwind that marks the end of the AGB phase may be highly asymmetric, and in the Interacting Stellar Wind model could

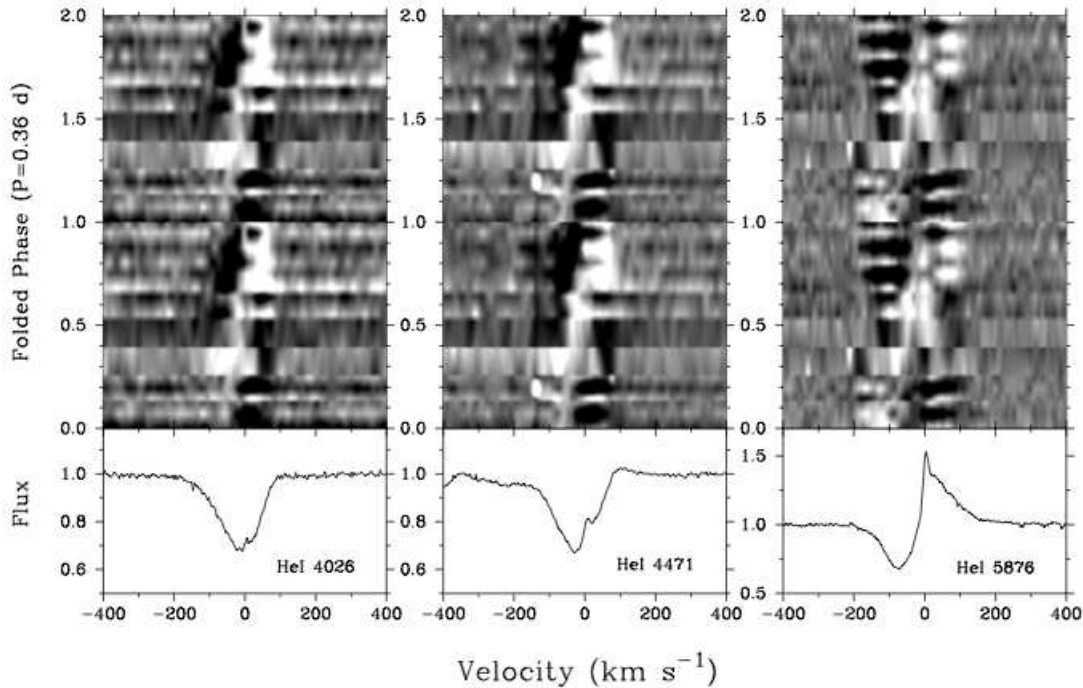


Figure 9. Individual He I $\lambda 4026$, He I $\lambda 4471$

and He I $\lambda 5876$ quotient spectra are shown phased over 2 cycles on a period of 0.36 days.

result in a non-spherical nebula. The young nebula of He 2-138 is undoubtedly complex (e.g. Sahai & Trauger 1998) and suggestive of strongly collimated post-AGB mass-loss. The morphology of the low and high ion UV lines presented here also points to an asymmetry in the subsequent central star wind. The cause of this asymmetry remains uncertain. The role of subsurface convection and a sustained AGB magnetic dynamo has been studied previously in the context of bipolar PN shapes (e.g. Blackmann et al. 2001; Nordhaus et al. 2007). The combination of rotation and a long-term large-scale magnetic field might then lead to an equatorially enhanced super-wind. Indeed our notion that the central star in He 2-138 may be a rapid rotator would be consistent with the simulations of e.g. Dwarkadas (2004), who reported that fast rotation of the central star can lead to non-spherical mass-loss. In the early stages of the nebular evolution the aspherical mass-loss could then result in a bipolar wind-blown bubble.

An alternative scenario is that binarity is the cause of the non-spherical planetary nebulae. Photometric and spectroscopic radial velocity surveys have suggested that at least $\sim 15\%$ of PN central stars are in short period (less than 3 days) close binaries (e.g. Bond 2000; De Marco et al. 2004). Unambiguous spectroscopic confirmation of central star binaries has been difficult to achieve and in many cases the fluctuations of deep-seated spectral lines appear to be erratic and not cyclic on a clear period (e.g. De Marco et al. 2008). In our study of He 2-138 the photospheric He I and metal lines are also variable, but they do not exhibit the tell-tale sinusoidal pattern in radial velocity shifts. We argue here instead that at least the \sim hourly temporal changes evident in the photospheric lines of He 2-138 are more reliably

interpreted as blue-to-red migrating features in the absorption profiles, which may provide tentative evidence for photospheric velocity fields and wave-leakage due to prograde non-radial pulsations. We would not assign the changes seen in e.g. He I $\lambda 4026$, He I $\lambda 4471$, and CIV $\lambda 5801$ as due to the effects of a variable central star *wind*. In He 2-138 the outflow is only diagnosed in our data via the P Cygni-like profiles of He I $\lambda 5876$ and the FUV and UV resonance lines.

Unravelling the occurrence of central star binarity and photospheric structures (pulsational or magnetic) demands intensive time-series over several days. These requisites are observationally challenging to secure, particularly as multi-site observations may also be needed in order to provide sufficiently continuous monitoring. However, we have demonstrated in this study of He 2-138 that it may be rewarding to conduct an extensive comparative study of the morphologies of the UV fast wind lines of young PN central stars, with the goal of investigating in time-averaged (archival) data the evidence for non-spherical outflows. These signatures may be relics of the structure of the preceding post-AGB super-wind phase.

ACKNOWLEDGMENTS

We are grateful for the support of staff at the European Southern Observatory, La Silla, Chile. Thanks also to Adam Burnley for his support of the ESO observing run. Finally, we would like to thank John Hillier for making the CMFGEN code available to us.

REFERENCES

- Bond, H. E. 2000, in ASP Conf. Ser. 199: Asymmetrical Planetary Nebulae II: From Origins to Microstructures, 115
- Afsar, M., Bond, H. E. 2005, Memorie della Societa Astronomica Italiana, 76, 608
- Blackman, E. G., Frank, A., Markiel, J. A., Thomas, J. H., Van Horn, H. M. 2001, Nature, 409, 485
- Cranmer, S. 1996, Ph.D. Thesis, University of Delaware
- De Marco, O., Bond, H.E., Harmer, D., Fleming, A.J. 2004, ApJ, 602, 93
- De Marco, O., Hillwig, T. C., Smith, A. J. 2008, AJ, 136, 323
- Dwarkadas, V.V., 2004, in Asymmetrical Planetary Nebulae III: Winds, Structure and the Thunderbird, Proceedings of the conference held 28 July - 1 August 2003 at Mt. Rainier, Washington, USA. eds. M. Meixner, J. H. Kastner, B. Balick and N. Soker. ASP Conference Proceedings, Vol. 313. San Francisco: Astronomical Society of the Pacific, 2004., p.430
- Fullerton, A.W., Gies, D.R., Bolton, C.T, 1996, ApJS, 103, 475
- Hillier, D.J., Miller, D., 1998, ApJ, 496, 407
- Hubeny, I., Lanz, T. 1995, ApJ, 439, 905
- Hutton, R.G., Mendez, R.G. 1993, A&A, 267, 8
- Kastner, J.H., Montez, R., Jr., Balick, B., De Marco, O. 2008, ApJ, 672, 957
- Kudritzki, R.P., Urbaneja, M.A., Puls, J. 2006, IAU Symp. 234, 'Planetary Nebulae in our Galaxy and Beyond', eds. M.J. Barlow & R.H. Mendez, CUP, 119.
- Lamers, H.J.G.L.M., Cerrutti-Sola, M., Perinotto, M. 1987, ApJ, 314, 726
- Massa, D., Fullerton, A.W., Sonneborn, G., Hutchings, J.B. 2003, ApJ, 586, 996
- Mendez, R.H., Forte, J.C., Lopez, R.H. 1986, Rev. Mex. Astron. Astrofis., Vol. 13, No. 2, 19
- Mendez et al. 1988, A&A, 190, 113
- Nordhaus, J., Blackman, E. G., & Frank, A. 2007, MNRAS, 376, 599
- Perinotto, M. 1987, IAU Symp. 131, 293
- Prinja, R.K., Hodges, S.E., Massa, D.L., Fullerton, A.W, Burnley, A.W. 2007, MNRAS, 382, 299
- Roberts, D.H., Lehar, J., Dreher, J.W. 1987, AJ, 93, 968
- Sahai, R., Trauger, J.T. 1998, AJ, 116, 1357
- Schneider, S.E., Terzian, Y., Purgathofer, A., Perinotto, M. 1983, ApJS, 52, 399
- Townsend, R.H.D. 2000, MNRAS, 318, 1
- Urbaneja, M.A., Kudritzki, R.-P., Puls, J., 2008, in Clumping in hot-star winds : proceedings of an international workshop held in Potsdam, Germany, 18. - 22. June 2007. Hamann, Wolf-Rainer (ed.) ; Feldmeier, Achim (ed.) ; Oskinova, Lidia M. (ed.). ISBN 978-3-940793-33-1., p.67
- Zhang, C.Y. 1995, ApJS, 98, 659
- Zickgraf, F.-J., Wolf, B., Stahl, O. 1985, A&A, 143, 421